

# DreamCAD: Scaling Multi-modal CAD Generation using Differentiable Parametric Surfaces

Muhammad Sadil Khan<sup>1,2†</sup> Muhammad Usama<sup>1,2</sup> Rolandos Alexandros Potamias<sup>3</sup>  
 Didier Stricker<sup>1,2</sup> Muhammad Zeshan Afzal<sup>1</sup> Jiankang Deng<sup>3</sup> Ismail Elezi<sup>4</sup>

<sup>1</sup> DFKI <sup>2</sup> RPTU, Kaiserslautern <sup>3</sup> Imperial College London  
<sup>4</sup> Huawei London Research Center



Figure 1. Our proposed **DreamCAD** (left) is a multimodal generative framework that can reconstruct editable CAD models from text, images, and point clouds using parametric patches. **CADCap-1M** (right) provides 1M+ GPT-5-generated captions.

## Abstract

Multimodal CAD generation faces a fundamental scalability challenge. Design-history methods are confined to small annotated datasets, while BRep topology is discrete and non-differentiable. Meanwhile, millions of unannotated 3D meshes remain untapped, since existing CAD methods cannot leverage them without explicit CAD annotations. We propose **DreamCAD**, a multimodal generative framework that bridges this gap by representing shapes as  $C^0$ -continuous Bézier patches with differentiable tessellation, enabling direct point-level supervision on large-scale 3D meshes without CAD-specific annotations. The resulting surfaces are exportable as STEP files

and editable in standard CAD software. We further introduce **CADCap-1M**, the largest CAD captioning dataset with 1M+ GPT-5-generated descriptions to advance text-to-CAD research. **DreamCAD** achieves state-of-the-art performance on ABC and Objaverse across text, image, and point modalities, surpassing 75% user preference. Finally, we demonstrate that **DreamCAD**'s accurate and compact geometric foundation enables topology recovery for production-ready CAD generation. Project page is available at <https://sadilkhan.github.io/dreamcad2026/>

## 1. Introduction

Computer-Aided Design forms the foundation of modern engineering [73], architecture, and manufacturing [28]. Unlike 3D meshes or point clouds that approximate geome-

<sup>†</sup>Work done during an internship at Huawei London Research Center.

try [59], CAD models are built from parametric primitives such as Bézier and NURBS surfaces, encoded in boundary representation (BRep) format, capturing both topology and precise geometry essential for industrial design [6]. With the advent of generative AI [10, 65], AI-assisted CAD generation [39] has become a promising frontier for accelerating design workflows and enabling rapid prototyping of manufacturable models [17].

Recent CAD generation methods enable multimodal synthesis from text [21], images [69], or point clouds [35]. However, achieving strong generalization across modalities and diverse geometries remains a major challenge. The root cause lies in the CAD representation and the training scheme. Design-history-based models [62] rely on *sketch-and-extrude* sequences from small datasets such as DeepCAD-160k [62] and Fusion360-8k [60], constraining the generalization in freeform or open-vocabulary shapes. UV and graph-based methods [67] require explicit BRep annotations, which are costly and difficult to scale. Although ABC [23] contains 1M BReps, it remains underutilized due to these bottlenecks.

In contrast, modern 3D generative models [71] scale effectively by decoupling mesh generation into multiple stages, using intermediate representations such as SDFs [47], or NeRFs [40]. We argue that scaling multimodal CAD generation requires an analogous paradigm shift - from single-stage joint geometry and topology generation to a decoupled pipeline. The first stage should focus on scalable parametric geometry leveraging unstructured 3D data without explicit CAD annotations, while subsequent stages can work toward recovering full CAD topology from this intermediate geometric foundation.

To address the first stage of generalizability, we propose **DreamCAD**, a multi-modal generative framework that produces editable parametric surfaces from point-level supervision alone. Each CAD model is represented as a set of rational Bézier patches defined by learnable control points and weights. These surfaces are differentially tessellated into meshes for point-based supervision via Chamfer loss. DreamCAD encodes sparse voxels into structured latents (SLAT) [65] to learn a CAD-oriented latent space, which is decoded into parametric geometry. Building on this, we adopt a coarse-to-fine conditional generation framework supporting *text*, *image*, and *point cloud* inputs.

A key challenge with patch-based BRep representations is ensuring  $C^0$  continuity, which is essential for valid CAD modeling.  $C^0$  continuity [11] requires adjacent surface patches to share common boundaries without gaps or overlaps. We address the continuity problem structurally rather than using any geometric optimization. Starting from a sparse voxel grid, we remove internal quads via flood-fill [12]. This way, each surface quad maps to a parametric

Dataset	Samples	CADCap	Dataset	Samples	CADCap
ABC [23]	757,433	✓	3D-Future [13]	16,990	✓
Automate [19]	380,124	✓	ModelNet [64]	12,308	✓
ShapeNet [4]	52,458	✗	ABO [5]	7,944	✗
CADParser [72]	40,989	✓	Fusion360 [60]	4,603	✓
HSSD [22]	30,078	✗	Toys4K [54]	3,482	✗
<b>Total</b>				<b>1,306,409</b>	

Table 1. Training datasets for DreamCAD comprising 1.3M 3D meshes. ✓denotes if the dataset is included in proposed CADCap-1M dataset.

patch initialized with control-point grids and unit weights, with adjacent patches sharing boundary points for continuity. The VAE decoder then refines control points and weights to match the target geometry. At inference, Bézier surfaces are exported as STEP files via OpenCascade [44]. Importantly, while the resulting STEP files do not contain industry-standard CAD topology, they are directly editable via control point and weight manipulation. In Section 5.4, we show that DreamCAD’s high-fidelity and compact geometric reconstruction can provide a strong geometric prior for topology recovery.

We curate over 1M 3D meshes from 10 publicly available datasets, as summarized in Table 1, to train our VAE architecture. For *text-to-CAD* training, existing datasets such as Text2CAD-160K [21] lack the scale and diversity necessary for robust generative modeling. To address this, we construct **CADCap-1M**, the largest CAD captioning dataset to date. We leverage GPT-5 to generate high-quality captions for 1M+ models from existing large-scale CAD datasets. We evaluate DreamCAD on multimodal generation tasks across *text*, *image*, and *point cloud* on both ABC [23] and Objaverse [7] datasets. Our experiments show that DreamCAD consistently surpasses baselines in both geometric accuracy and user preference. Our contributions are as follows

1. We introduce **DreamCAD**, a multi-modal generative framework trained only with point supervision without any dependence on CAD annotations.
2. We release **CADCap-1M**, the largest CAD captioning dataset with over 1M text descriptions for scalable text-to-CAD research.
3. DreamCAD achieves state-of-the-art performance across *point-*, *image-*, and *text-conditioned* generation tasks, reducing Chamfer Distance by up to 70% in *point-to-CAD* and surpassing 75% preference in expert and GPT-based evaluations for *text* and *image-to-CAD*.

## 2. Related Work

**Generative CAD.** Prior CAD generative models [26, 55, 62] represent geometry through boundary representations (BReps), which offer exact, watertight, and editable geometry but are difficult to learn at scale due to their complex parametric and topological structure [15]. Existing approaches therefore struggle to balance scalability with geo-

metric fidelity.

Design-history methods [21, 50, 62] model CAD creation using *sketch-extrude* operations, framed as program synthesis [50, 58, 66, 72] or language modeling [9, 20, 31, 38]. However, they require design-history logs available only in proprietary CAD softwares [2, 43]. This limits training to small datasets (e.g., DeepCAD-170K [62], Fusion360-8K [60]) and models exhibit poor generalization to complex, real-world geometries [14, 58].

Some works model BReps through UV parameterizations or hierarchical graph structures since explicit BRep topology (e.g. vertices, edges, faces) is discrete and non-differentiable, preventing gradient-based optimization for geometry based learning. UVNet [18] and DTG-BRepGen [30] predict UV grids from face annotations, while BRepGen [67] and BRepDiff [27] perform UV-space diffusion with post-processing. However, these methods face some key limitations: (i) no guaranteed  $C^0$  continuity across adjacent faces, (ii) training restricted to models with fewer faces [27], excluding  $\sim 70\%$  of ABC [23], (iii) BRep conversion requires expensive grid-based fitting stages with high error and invalidity rate [1, 15], and (iv) UV parameterizations only approximate geometry with resolution-related computational challenges. Self-supervised methods [32, 49, 56] attempts to learn CAD geometry without using any CAD annotation. However, these methods either do not scale well or restrict to simpler shapes and have never been explored for multimodal purposes. Similarly, surface-fitting approaches [35, 51, 61] require slow per-sample optimization, unsuitable for scalable generation. NURBGen [55] takes a promising direction by framing BRep generation as a sequence modeling task using symbolic NURBS, enabling text-to-CAD via LLM fine-tuning. However, generating 3D geometry directly from text without visual grounding leads to low fidelity [52, 53] on complex or geometrically precise prompts.

While industry-standard BRep topology remains the gold standard for professional CAD workflows, directly training on BReps from multimodal inputs is neither scalable nor viable, as the above limitations collectively prevent gradient-based learning on large-scale BRep data. Inspired by recent progress in 3D generation [52, 70], we argue that scalable CAD synthesis requires a decoupled two-stage pipeline: a first stage that learns generalizable 3D shape from large-scale unstructured data, and a second stage that recovers fine-grained CAD topology from these intermediate representations. DreamCAD addresses the first stage via  $C^0$ -continuous Bézier patches with differentiable tessellation, enabling point-level supervision on large-scale 3D meshes without CAD-specific annotations.

**Multimodal CAD Datasets.** Unlike 3D vision, where large-scale multimodal datasets such as Objaverse [7] and

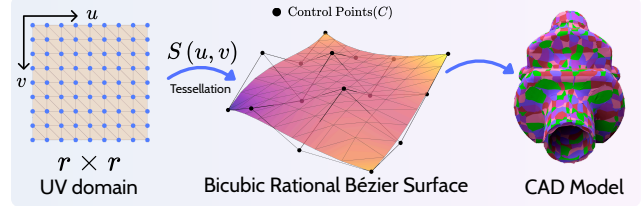


Figure 2. Bézier surface representation and differentiable tessellation.

MARVEL-40M+ [53] have driven progress in text-to-3D generation, the CAD domain remains limited by multimodal data scarcity. Existing CAD datasets, such as Text2CAD-160K [21], contain design histories with text captions but are small in scale. Moreover, large-scale CAD datasets such as ABC-1M [23] and Automate-440K [19] lack textual or visual descriptions, restricting their use for multimodal generative learning. Although recent advances in automated 3D captioning, including Cap3D [37] and MARVEL-40M+ [53], have enabled large-scale annotations for meshes, there are still no comparable resources for BRep models. To bridge this gap, we introduce **CADCap-1M**, a dataset of over 1M high-quality text descriptions for CAD models automatically generated using GPT-5, for scalable training and evaluation for text-to-CAD research.

### 3. Preliminaries

In this section, we briefly review the CAD representation used in the DreamCAD architecture. Among the various parametric surface formulations, Bézier and NURBS are the most widely adopted in modern CAD modeling. In our implementation, we choose bicubic rational Bézier surfaces due to their conceptual simplicity and analytical tractability. Furthermore, rational Bézier surfaces can be viewed as a special case of NURBS surfaces, making them naturally compatible with standard CAD operations.

**Rational Bézier Surface:** A rational Bézier surface of degree  $(n, m)$  is defined by  $(n + 1) \times (m + 1)$  control points  $C = \{c_{ij}\}$  and non-negative weights  $W = \{w_{ij}\}$ . The surface  $S(u, v)$  is evaluated in  $uv$  domain as:

$$S(u, v) = \frac{\sum_{i,j} B_i^n(u) B_j^m(v) w_{ij} c_{ij}}{\sum_{i,j} B_i^n(u) B_j^m(v) w_{ij}}, \quad (1)$$

where  $B_i^n(u) = \binom{n}{i} u^i (1-u)^{n-i}$  and  $B_j^m(v) = \binom{m}{j} v^j (1-v)^{m-j}$  are Bernstein basis functions and  $(u, v) \in [0, 1]^2$ . For a bicubic case  $n = m = 3$ . This formulation is differentiable with respect to both control points and weight. It is worth noting that the weights  $w_{ij}$  must remain non-negative, as negative weights can lead to degenerate or invalid surface evaluations.

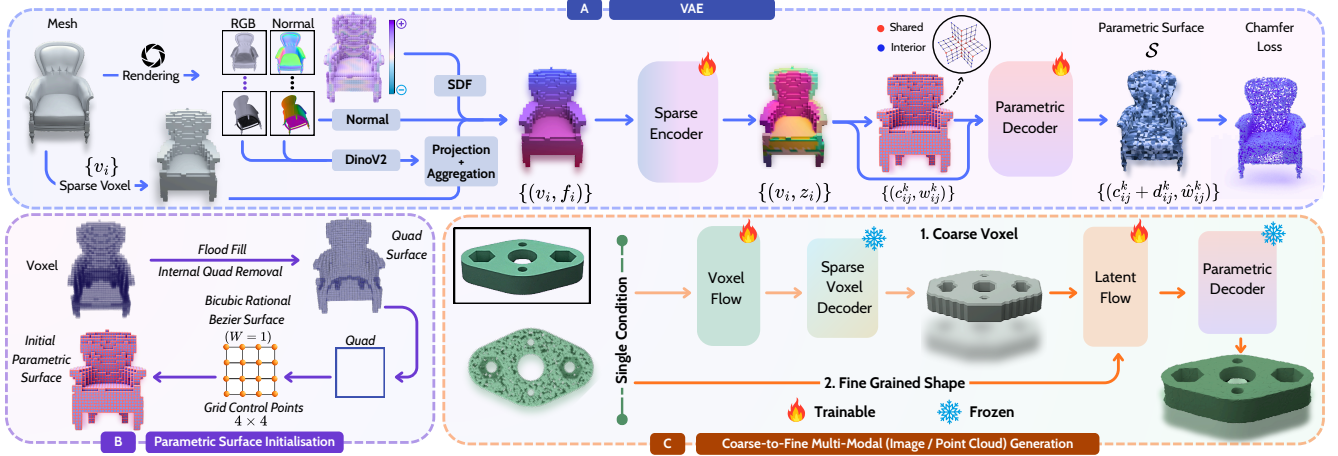


Figure 3. **DreamCAD Overview:** (A). **Sparse Transformer VAE** takes as input mesh, generates active voxels  $v_i$  with local features  $f_i$ , from DINOv2 [46] embeddings, normal images, and SDF values and encodes it to generate structured latents  $z_i$ . These are then decoded into parametric (rational bézier) surfaces and optimized using Chamfer loss. (B). **Initial  $C^0$ -continuous Parametric Surface** generation from sparse voxels via flood-fill and quad conversion using grid control points and unit weights. (C). **Multi-modal CAD generation** from images, or points using a coarse-to-fine flow-matching framework from coarse voxel grid to parametric surface refinement.

**Differentiable Mesh Generation:** Given a set of Bézier patches  $\{S_k\}_{k=1}^K$ , we generate meshes through differentiable tessellation [61] (Figure 2). Each patch  $S_k(u, v)$  is evaluated on the  $uv$  domain by uniformly sampling  $(u, v)$  points on a grid of resolution  $r \times r$ . Adjacent points in this grid define quadrilateral cells, which are then split into triangles to form a locally consistent mesh. Neighboring Bézier patches are merged along shared boundaries to ensure  $C^0$  connectivity.

Since  $S(u, v)$  is differentiable with respect to its  $C$  and  $W$ , the entire tessellation process supports end-to-end gradient-based optimization.

## 4. Methodology

As shown in Figure 3, **DreamCAD** adopts a multi-stage generative pipeline. Section 4.1 presents the VAE module, which encodes 3D shapes into compact latent representations and decodes them into a parametric surface. Section 4.2 details the automatic captioning pipeline. Finally, Section 4.3 introduces the conditional generation framework, which uses a coarse-to-fine strategy: sparse voxels are first generated from the input condition, followed by reconstruction of fine-grained parametric surfaces.

### 4.1. Latent Encoding

**Sparse Voxel Representation.** An effective 3D encoder requires a compact yet structured representation. While point clouds are widely used [33, 71], they lack spatial regularity for continuous CAD generation. We instead adopt a sparse voxel representation enriched with local visual features [65]. We first voxelize each input mesh to  $32^3$  resolu-

tion, generating active voxels  $\{v_i\}_{i=1}^N$ . To preserve fine geometric details, each active voxel is augmented with visual cues. We render 150 RGB and normal views of the mesh from different camera angles, extract DINOv2 [46] embeddings, and project each voxel center  $v_i$  to obtain per-view RGB and normal features. Averaging across views gives:

$$p(v_i) = \frac{1}{150} \sum_{j=1}^{150} \left[ \text{proj}(v_i, E_j^r); \text{proj}(v_i, E_j^n) \right], \quad (2)$$

where  $\text{proj}$  is the projection operator and  $p(v_i)$  is the mean feature vector,  $E_j^r$  and  $E_j^n$  are DINO embedding maps from the  $j$ -th RGB and normal views. We further include per-view normals  $n(v_i) \in \mathbb{R}^{150 \times 3}$ , voxel centers  $c(v_i) \in \mathbb{R}^3$ , and signed distance values  $s(v_i) \in \mathbb{R}$  to encode geometry and surface proximity. The final voxel feature is:

$$f_i = [p(v_i); n(v_i); c(v_i); s(v_i)], \quad f_i \in \mathbb{R}^{2502} \quad (3)$$

These features are processed by a sparse Transformer encoder [65] to produce structured latents  $\{(v_i, z_i)\}_{i=1}^N$ .

**Initial Parametric Quad Generation:** The goal of the decoder is to reconstruct the 3D shape as a set of Bézier patches from the structured latent codes. Each patch requires 16 control points and corresponding weights. Directly generating these parameters from latents  $z_i$  will lead to disconnected or overlapping patches, as losses alone cannot enforce  $C^0$  continuity between two adjacent patches.

To mitigate this, we generate an initial parametric quad surface from sparse voxels (Fig. 3.B). First, we generate a surface mesh from the sparse voxels using a flood-fill algorithm, which removes the internal quads from the voxels.

We then convert each quad into a bicubic rational bézier patch by uniformly sampling a  $4 \times 4$  grid points using bilinear interpolation of its four corners.

All control points start with unit weights, and adjacent patches share boundary control points (“• Shared” in Figure 3.A) to ensure  $C^0$  continuity. The resulting surface  $S$  is represented as:

$$\mathcal{S} = \{s_k = (c_{ij}^k; w_{ij}^k)\} \in \mathbb{R}^{N_f \times 16 \times 4}, \quad (4)$$

$$k \in \mathbb{Z}_{[0, N_f]}, \quad i, j \in \{0, 1, 2, 3\},$$

where  $N_f$  denotes the number of patches,  $s_k$  denotes the  $k^{\text{th}}$  patch and  $i, j$  are the indices for both control points and weights. In practice, we observe that the number of patches per shape remains low, typically  $N_f \ll 10000$ .

**Parametric Surface Decoder:** The decoder refines the initial surface  $S$  by using structured latent features to predict local adjustments for each patch. For the  $(i, j)$ -th control point of the  $k$ -th patch, it predicts a deformation  $d_{ij}^k$  and a weight update  $\hat{w}_{ij}^k$ . Unconstrained  $d_{ij}^k$  often causes degenerate geometries such as spikes or self-intersections, which are hard to recover during optimization. Therefore, to stabilize training, we bound the deformation within a local neighborhood using  $c_{ij}^k \leftarrow c_{ij}^k + \tanh(d_{ij}^k)$ . We ensure positive weights via the softplus function  $\log(1 + e^{\hat{w}_{ij}^k})$ . For shared boundary control points, we enforce  $C^0$  continuity by uniformly averaging the predicted deformations and weight updates from all patches sharing that point, ensuring all adjacent patches converge to the same boundary position.

We then tessellate the deformed surface into a mesh and compute Chamfer distance (CD) loss between sampled surface points ( $\mathcal{X}_d$ ) and the target point cloud ( $\mathcal{X}_g$ ). The overall training objective is:

$$\mathcal{L} = \lambda_{cd} \text{CD}(\mathcal{X}_g, \mathcal{X}_d) + \lambda_{g1} \text{G1}(\mathcal{S}_d) + \lambda_{lp} \text{Laplacian}(\mathcal{M}_d) + \lambda_{kl} D_{KL}, \quad (5)$$

where  $\mathcal{M}_d$  is the tessellated mesh from  $\mathcal{S}_d$ , G1 [8] enforces tangent continuity between two adjacent patches, Laplacian [42] ensures smoothness and  $D_{KL}$  regularizes the VAE latent space using KL divergence loss. We provide additional details in the supplementary material.

## 4.2. CADCap-1M Dataset

Recent progress in text-to-3D generation has been driven by large-scale captioned datasets such as MARVEL-40M+ [53] and Cap3D [37], yet no comparable resource exists for *text-to-CAD*. To progress the field, we introduce CADCap-1M, comprising 1M+ high-quality captions for CAD models from ABC [23], Automate [19], CADParser [72], Fusion360 [60], ModelNet [64], 3D-Future [13]. For each model, we render four orthographic



Figure 4. Examples of metadata-augmented captions from CADCap-1M showing object type, part names, and hole counts.

views using Blender [3] and prompt GPT-5 [45] to generate concise descriptions. Prompts are augmented with metadata from the original CAD files, such as model names which are optionally extracted from *.step* files, number of holes, which is computed using [41], and relative dimensions (*length-to-width*, *width-to-height*, or *length-to-height* ratios). This metadata-augmented prompting substantially reduces hallucinations and improves geometric accuracy and linguistic quality [21, 53]. As a result, CADCap-1M produces more shape-centric and structure-aware captions (e.g., “M3x8 bolt ..”, “.. mounting plate .. 40 circular holes ..”), as illustrated in Figure 4.

## 4.3. Conditional CAD Generation

We now describe the process of conditional CAD generation from text, images, and point clouds.

**Generation Pipeline:** As shown in Figure 3.C, DreamCAD adopts a coarse-to-fine generation pipeline with two Flow Transformer Decoders optimized via flow matching (FM) objectives [34]. FM learns to estimate velocity field  $v_\theta(x_t, t)$  for transforming samples from a prior distribution  $x_0 \sim p_0$  to the target distribution  $x_1 \sim p_1$  through the loss  $\mathcal{L}_{\text{FM}} = \mathbb{E}_{x_0, x_1, t} [\|v_\theta(x_t, t) - (x_1 - x_0)\|_2^2]$ .

In the first stage, we generate a coarse voxel grid from the input condition by producing a low-resolution latent structure through a lightweight VAE trained to reconstruct voxel grids, following [65]. The pretrained VAE decoder efficiently upsamples this latent grid into a full-resolution voxel representation. In the second stage, we generate local SLAT features ( $z_i$ ) for each active voxel ( $v_i$ ) using the predicted voxel grid and conditioning input. Finally, the pretrained parametric surface decoder transforms  $\{(v_i, z_i)_{i=1}^N\}$  into the final parametric surface  $\mathcal{S}$ . For conditional embedding, we use modality-specific encoders: DINOv2 [46] for images

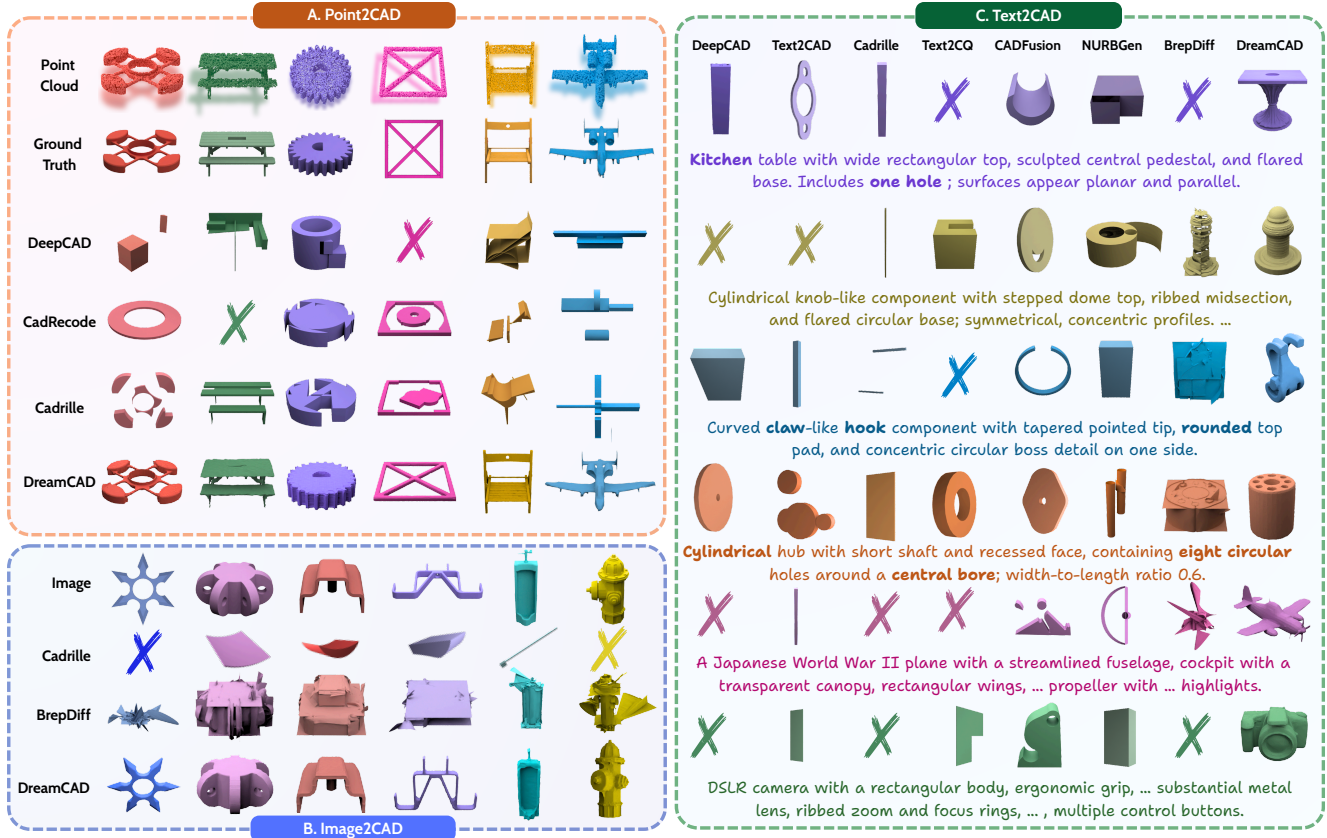


Figure 5. Qualitative comparison on **Point2CAD** (Top-Right), **Image2CAD** (Bottom-Left) and **Text2CAD** (Right) tasks. For each task, the first four examples are from the ABC dataset, while the last two from Objaverse dataset. **X** indicates invalid models.

and PointNet++ [48] for point clouds. We use pretrained weights for DINOv2 while training PointNet++ jointly with the Flow Transformer models.

**Text-to-CAD Generation:** While our framework supports text conditioning, training a direct text-to-3D model typically leads to slow convergence [52] and low prompt fidelity [53], due to the lack of explicit spatial and geometric cues in textual input. Following standard text-to-3D practices [29, 52, 53, 70], we adopt a two-stage approach: *text-to-image* followed by *image-to-CAD*. We fine-tune Stable Diffusion 3.5-2B [10] on the CADCap-1M dataset to align its output image distribution with that of the *image-to-CAD* model [53]. The resulting images are then used to condition our pretrained *image-to-CAD* model. This significantly enhances prompt fidelity with reduced training cost. Notably, pretrained *text-to-image* models [10, 25] often fail to preserve numerically constrained features such as hole or gear-tooth counts, underscoring the importance of fine-tuning for accurate *text-to-image* generation for the CAD domain.

## 5. Experiments

We evaluate DreamCAD on conditional CAD generation from text, image, and point inputs in Section 5.1. Sec-

tion 5.2 analyzes the caption quality of the CADCap-1M dataset, and Section 5.3 presents ablation studies on key architectural and training design choices.

**Datasets:** We curate over 1M high-quality CAD models from 10 public datasets (Table 1) to train the DreamCAD VAE, converting all BRep-only datasets to meshes using OpenCascade. Although large-scale datasets like ABC and Automate contain BReps, training directly on BReps is impractical at scale as BRep topology is discrete and non-differentiable. We filter low-quality and trivial primitives from ABC [23] and Automate [19], splitting into 95% training, 2.5% validation, and 2.5% testing. For *text-to-CAD*, we use CADCap-1M and MARVEL [53] Level-5 captions for ShapeNet [4], Toys4K [54], and ABO [13]. For *image-to-CAD*, we render four orthographic views (front, back, left, right) in Blender [3] and randomly sample one view per epoch. For *point-to-CAD*, we normalize point clouds to  $[-0.5, 0.5]$  and augment with surface normals in 50% of batches. We discuss more details in the supplementary.

**Implementation:** We train DreamCAD VAE for 700k steps for 3 weeks with batch size 32 using mixed-precision, AdamW [36] with learning rate  $5 \times 10^{-5}$  and weight decay  $1 \times 10^{-4}$ . Both VAE encoder and decoder contain 8 Trans-

Task	Models	ABC							Objaverse						
		F1 ↑	NC ↑	CD ↓	HD ↓	JSD ↓	MMD ↓	IR ↓	F1 ↑	NC ↑	CD ↓	HD ↓	JSD ↓	MMD ↓	IR ↓
Point2CAD	DeepCAD [62]	19.31	0.49	51.10	0.37	783.94	29.63	11.01	7.05	0.48	320.33	0.41	855.14	34.62	10.88
	CAD-Recode [50]	75.99	0.79	3.73	0.13	271.89	2.94	15.39	53.24	0.66	7.92	0.19	479.50	6.27	15.53
	Cadrille [24]	78.86	0.80	2.98	0.12	236.10	2.51	5.84	57.49	0.67	6.28	0.17	445.23	5.24	10.81
	<b>DreamCAD (Ours)</b>	<b>92.12</b>	<b>0.94</b>	<b>0.93</b>	<b>0.06</b>	<b>96.13</b>	<b>0.84</b>	<b>0.00</b>	<b>87.31</b>	<b>0.89</b>	<b>1.25</b>	<b>0.11</b>	<b>189.12</b>	<b>1.86</b>	<b>0.00</b>
Img2CAD		GPT ↑	User ↑	CD ↓	HD ↓	JSD ↓	MMD ↓	IR ↓	GPT ↑	User ↑	CD ↓	HD ↓	JSD ↓	MMD ↓	IR ↓
	Cadrille [24]	7.75	5.34	111.50	0.49	909.92	68.97	14.19	1.10	0.45	99.91	0.48	913.24	58.02	27.16
	BRepDiff [27]	16.13	17.63	20.69	0.28	662.97	13.89	0.11	18.12	16.63	57.51	0.43	875.68	27.83	0.96
	<b>DreamCAD (Ours)</b>	<b>76.12</b>	<b>77.03</b>	<b>4.12</b>	<b>0.17</b>	<b>412.31</b>	<b>6.31</b>	<b>0.00</b>	<b>80.78</b>	<b>82.92</b>	<b>20.16</b>	<b>0.27</b>	<b>541.81</b>	<b>13.41</b>	<b>0.006</b>
Text2CAD		GPT ↑	User ↑	CD ↓	HD ↓	JSD ↓	MMD ↓	IR ↓	GPT ↑	User ↑	CD ↓	HD ↓	JSD ↓	MMD ↓	IR ↓
	DeepCAD [62]	0.49	0.40	86.54	0.44	887.69	37.66	39.02	0.00	0.00	80.68	0.45	903.40	37.34	41.9
	Text2CAD [21]	1.11	2.46	82.22	0.41	852.68	40.65	6.43	0.22	0.36	93.96	0.47	896.22	44.79	9.37
	Cadrille [24]	0.91	0.34	155.80	0.53	957.51	96.89	4.44	0.04	0.00	162.16	0.55	961.53	76.39	6.55
	Text2CQ [66] (Qwen3B)	0.01	0.00	68.15	0.39	829.72	37.50	12.52	0.00	0.00	83.43	0.44	890.89	47.62	14.4
	Text2CQ (GPT2L)	0.02	0.00	71.27	0.39	838.54	40.35	34.05	0.00	0.00	84.85	0.47	891.96	53.70	64.25
	Text2CQ (CodeGPT)	0.94	1.00	77.91	0.41	850.23	43.71	32.56	0.24	0.12	86.75	0.46	879.57	58.48	25.14
	CADFusion [57]	2.35	2.76	56.36	0.31	789.12	27.54	9.21	2.67	2.35	81.03	0.43	853.43	58.11	12.4
	NURBGen [55]	4.21	4.44	50.84	0.32	800.46	29.53	9.12	8.18	7.28	73.54	0.41	839.08	38.69	2.67
	BRepDiff [27]	4.34	3.20	54.12	0.38	812.31	34.72	1.12	6.33	6.41	74.32	0.38	808.19	41.13	2.31
	<b>DreamCAD (Ours)</b>	<b>85.62</b>	<b>85.40</b>	<b>20.32</b>	<b>0.14</b>	<b>734.92</b>	<b>19.43</b>	<b>0.00</b>	<b>82.32</b>	<b>83.48</b>	<b>34.61</b>	<b>0.28</b>	<b>698.21</b>	<b>28.14</b>	<b>0.00</b>

Table 2. Quantitative comparison on Point2CAD, Text2CAD, and Img2CAD tasks over the ABC and Objaverse datasets. F1 and IR are scaled by  $10^2$ , while CD, JSD, and MMD are scaled by  $10^3$ . For *text* and *image-to-CAD*, GPT and User ratings measure visual alignment.

former layers with voxel latent dimension  $z_i = 8$ . We empirically set the loss weights in Eq. 5 to  $\lambda_{cd} = 10^2$ ,  $\lambda_{g1} = 5 \times 10^{-3}$ , and  $\lambda_{lp} = 1$ . During training, points for CD loss increase from 16K to 100K via sigmoid scheduling and tessellation resolution  $r$  increases from (4, 4) to (16, 16). We train both coarse and fine-grained flow Transformer decoders for 500k steps with 10% condition dropout. Pre-trained image embeddings have a dimensionality of 1536. During inference, we use 50 steps and set the classifier free guidance scale to 7.5. For Stable Diffusion fine-tuning (text to image), we apply LoRA [16] with rank and  $\alpha=4$ , trained for 300k steps. Inference takes  $\sim 15$ s for *image-* and *point-to-CAD*, and  $\sim 30$ s for *text-to-CAD*.

## 5.1. Multimodal Generation Evaluation

**Experimental Setup.** We evaluate DreamCAD on two datasets: ABC [23] and Objaverse [7], each containing 15K samples. ABC serves as the in-distribution benchmark, while Objaverse is used for out-of-distribution (OOD) evaluation to measure generalization. Because Objaverse includes many free-form and organic objects uncharacteristic of CAD geometry, we filter its test set using MARVEL [53] captions containing CAD-specific keywords.

**Baselines:** As the first CAD generative framework trained on large-scale unstructured 3D data, DreamCAD has no direct counterparts. We therefore compare against representative design-history and UV-based methods across all tasks. For *text-to-CAD*, we include Text2CAD [21], Text2CQ [66], Cadrille [24], DeepCAD [62], CADFusion [57], NURBGen [55] and BRepDiff [27]. For CAD-Fusion [57], we generate 5 outputs per sample as per the of-

ficial implementation. We observe this drastically reduces the invalidity ratio. For the *image-to-CAD* task, we compare DreamCAD against BRepDiff and Cadrille while for the *point-to-CAD* we additionally include DeepCAD and CAD-Recode [50]. DeepCAD is trained for 100 epochs on both *point* and *text-to-CAD* tasks on DeepCAD and Text2CAD datasets, while BRepDiff is trained for *image-to-cad* for 6k epochs on ABC. Since the training schemes introduce a data-scale disparity, we additionally report results on the DeepCAD dataset in the supplementary.

**Metrics:** We evaluate all tasks using both geometric and perceptual metrics. Geometric fidelity is assessed by Chamfer Distance (CD), Hausdorff Distance (HD), Jensen–Shannon Divergence (JSD), Minimum Matching Distance (MMD), Normal Consistency (NC), F1 score, and Invalidity Ratio (IR), which quantifies the fraction of non-convertible BRep outputs. All geometric metrics are computed on 8192 uniformly sampled points normalized within a unit cube centered at the origin. For *text-* and *image-to-CAD*, visual alignment is measured on 5k and 1k samples through GPT-5 [63] and user studies by 14 CAD-experts, respectively. In both settings, GPT-5 and human evaluators are shown multi-view renderings of reconstructions from all baselines and DreamCAD, and asked to select the model best matching the input (*text* or *image*). The same expert group is used consistently across all user studies.

**Results:** As shown in Table 2, DreamCAD achieves state-of-the-art results across all three modalities in *point-to-CAD*, *image-to-CAD*, and *text-to-CAD*. In the easier *point-to-CAD* task, it outperforms baselines on ABC by a large

Model	CD ( $\times 10^3$ ) $\downarrow$	Lap ( $\times 10^3$ ) $\downarrow$	HD $\downarrow$
No Regularization	<b>0.0210</b>	0.0073	<b>0.02</b>
+G1	0.0230	0.0064	0.022
+Lap	0.0225	0.0022	0.022
+G1+Lap	0.0259	<b>0.0020</b>	0.024

(a) Impact of regularizers on VAE performance.

Voxel-Grid	24	32	48	64
#patches	1434.32	2546.18	7720.48	10179.34
CD ( $\times 10^3$ )	0.0231	0.011	0.0109	0.0105

(b) Ablation on voxel-grid resolution.

Table 3. Ablation studies on regularization (top) and voxel resolution (bottom).

margin, reducing CD by up to 68% and 75% over Cadrille and CAD-Recode and improving F1 scores by 17% and 21%, respectively, while attaining a zero invalidity ratio. Similar gains are observed across other metrics and the Objaverse dataset as well. As illustrated in Figure 5.A, DreamCAD accurately reconstructs complex geometries such as gear wheels (Ex. 3) and chair (Ex. 5), plane (Ex. 6), whereas prior methods capture only the coarse shapes.

For *image-to-CAD*, DreamCAD achieves over 75% preference in both GPT and human evaluations on ABC and Objaverse, improving CD by 80% and 58% and MMD by 54% and 52% over BRepDiff, respectively. As shown in Figure 5.B, DreamCAD produces high-fidelity reconstructions from single images via its coarse-to-fine pipeline and achieves the lowest invalidity ratio, failing only when no active voxels are generated in the coarse stage.

For the most challenging *text-to-CAD* task, DreamCAD attains over 80% preference in both GPT and user studies, substantially outperforming all baselines. The closest competitor, BRepDiff, which takes as input the same images generated by our finetuned SD 3.5, remains far behind in reconstruction quality. Geometrically, DreamCAD achieves a 62% reduction in CD with a zero invalidity ratio in the ABC dataset. As shown in Figure 5.C, it exhibits strong prompt fidelity, accurately reconstructing intricate shapes (Ex. 1: table, Ex. 6: camera) and numerically constrained features (Ex. 4: hole counts). Design-history-based models fail beyond simple primitives, while NURBGen’s lower prompt fidelity demonstrates that end-to-end text-to-CAD without visual grounding struggles to capture precise geometric details. Furthermore, BRepDiff’s post-processing stage occasionally produces disconnected BRep faces and visible spike artifacts from misplaced UV grid points, a limitation of grid-based representations that prevents reliable  $C^0$  continuity.

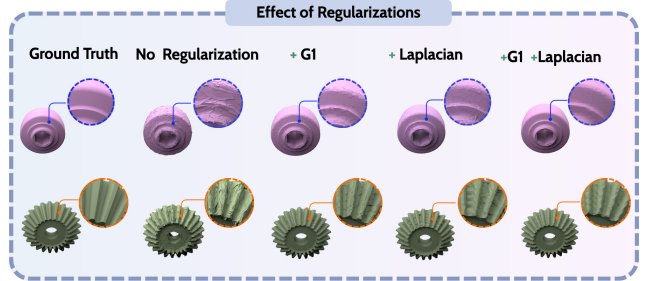


Figure 6. Examples showing VAE reconstructions for different regularizers.

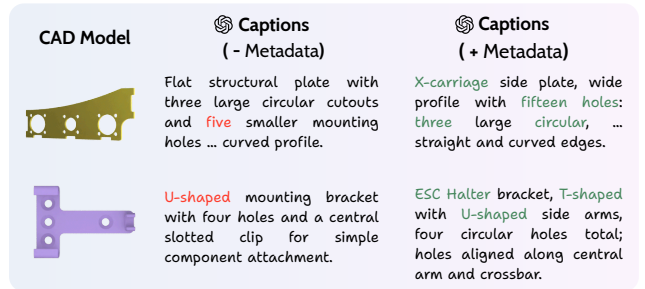


Figure 7. Comparison of captions produced by GPT-5 with and without metadata-augmented prompting, showing more geometrically faithful captions when metadata is included.



Figure 8. Comparison of images generated from the pretrained and fine-tuned SD-3.5 given same text prompts.

## 5.2. Caption Quality

As **CADCap-1M** is the first large-scale captioning dataset for CAD models, no existing benchmark enables direct comparison. We therefore evaluate caption quality through both user studies and GPT-5 assessment on 1k and 5k samples respectively. Given four rendered views, metadata, and the caption, evaluators rate both geometric and semantic accuracy. Overall, 95.8% (user) and 98.31% (GPT-5) of captions are judged correct, including precise identification of part names and hole counts. This validates the reliability of our metadata-augmented prompting. We provide more statistical analyses in the supplementary material.

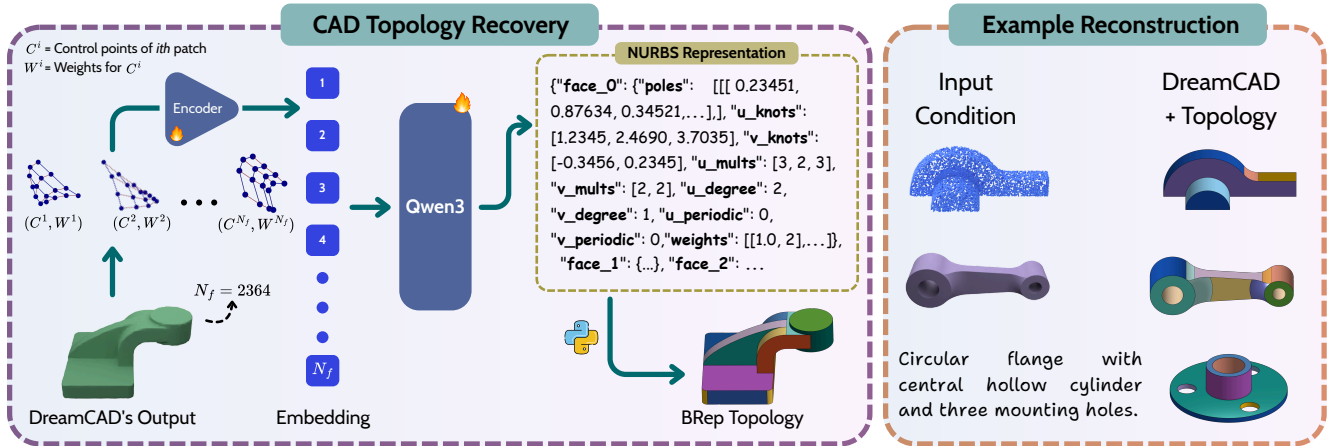


Figure 9. (Left) Topology recovery from patch-based outputs to hybrid NURBS CAD representation [55]. (Right) For multimodal inputs, DreamCAD reconstructions and the corresponding recovered topology.

### 5.3. Ablation Study

**Regularizations:** We analyze the impact of G1 and Laplacian regularizers on VAE reconstructions. We train the VAE from scratch on 300K samples and evaluating on 15K ABC test shapes (Table 3a and Figure 6). Without regularization, CD is minimized aggressively but produces rough surfaces with spike artifacts, reflected in the highest Laplacian value. Adding G1 or Laplacian individually improves smoothness, with Laplacian better preserving curvature. Combining both gives the lowest Laplacian loss (0.0020) and smoothest surfaces while maintaining strong geometric accuracy.

**Voxel-Grid Resolution:** We ablate the voxel-grid resolution used to initialize the parametric surfaces (Table 3.b). Since retraining the VAE at each resolution is expensive, we instead optimize 1000 randomly sampled training meshes. For each resolution, we voxelize each mesh, initialize the parametric surfaces, and optimize for 2000 epochs with learning rate  $10^{-4}$  and loss from Eq 5, supervised by ground-truth points. Increasing resolution from 32 to 48 and 64 increases patch count by  $3\times$  and  $4\times$ , while improving CD by only 1% and 5%. We therefore adopt resolution 32 as the best quality–efficiency trade-off.

**Metadata Augmentation:** We caption 1,000 random samples with and without metadata using GPT-5. Users preferred captions with metadata in 80.3% of cases, with more accurate part names and hole counts (Figure 7).

**Fine-Tuning Text-to-Image Model:** We compare 500 images generated by pretrained and fine-tuned Stable Diffusion models. User studies show that the fine-tuned model is preferred in 75.6% of cases, demonstrating a notable improvement in prompt fidelity (Figure 8).

### 5.4. Application: CAD Topology Recovery

While DreamCAD’s outputs are editable via control points and weights, they still lack complete CAD topology. This remains an open challenge and forms the basis of our future work. To explore feasibility, we fine-tune Qwen3-4B [68] with LoRA [16] on 50K samples to convert patch-based outputs into structured NURBS representations with semantic topology, following NURBGen [55]. Each patch is represented as 16 control points with weights, encoded via a Transformer encoder, and passed to Qwen3 for NURBS sequence prediction (Figure 9 - Left). Since patch counts remain low (e.g.,  $N_f = 2364$  in Figure 9), training is computationally tractable. Evaluated on 600 test samples across all three tasks (point-, image-, and text-to-CAD, 200 each), this generates 99.2% valid CAD models (Figure 9 - Right) with  $CD = 0.17 \times 10^{-3}$ . These results suggest that accurate and compact geometric reconstruction can provide a strong foundation for topology recovery for production-ready CAD generation. Full details are in the supplementary.

## 6. Conclusion

We present **DreamCAD**, a multi-modal generative framework that produces editable parametric surfaces directly from point-level supervision. Our goal is to address the long-standing challenge of generalizability in CAD generation. DreamCAD leverages a parametric patch-based CAD representation that supports differentiable mesh generation and enables point-based supervision for 3D shape synthesis. By removing the need for CAD-specific ground-truth annotations, our framework scales to large-scale 3D datasets for CAD geometry generation. In addition, we introduce **CADCap-1M**, the largest captioning dataset with high-quality textual descriptions generated using GPT-5

for advancing text-to-CAD research. Trained on 1M+ 3D meshes curated from 10 public datasets, DreamCAD demonstrates strong generalization across text, image, and point-conditioned generation tasks. While complete CAD topology recovery remains a hard and open problem, we view DreamCAD as establishing the geometric foundation upon which this challenging next stage can be built.

## 7. Acknowledgement

This work was in parts supported by the EU Horizon Europe Framework under grant agreement 101135724 (LUMINOUS).

## References

- [1] Sk Aziz Ali, Mohammad Sadil Khan, and Didier Stricker. Brep boundary and junction detection for cad reverse engineering. In *ICMI*. IEEE, 2024. 3, 14
- [2] Autodesk Inc. Autodesk Fusion 360: Integrated cad, cam, and cae software. <https://www.autodesk.com/products/fusion-360/>, 2024. 3
- [3] Blender Online Community. Blender – a 3d modelling and rendering package. <https://www.blender.org/>, 2025. 5, 6
- [4] Angel X Chang, Thomas Funkhouser, Leonidas Guibas, Pat Hanrahan, Qixing Huang, Zimo Li, Silvio Savarese, Manolis Savva, Shuran Song, Hao Su, et al. Shapenet: An information-rich 3d model repository. *arXiv:1512.03012*, 2015. 2, 6
- [5] Jasmine Collins, Shubham Goel, Kenan Deng, Achleshwar Luthra, Leon Xu, Erhan Gundogdu, Xi Zhang, Tomas F Yago Vicente, Thomas Dideriksen, Himanshu Arora, Matthieu Guillaumin, and Jitendra Malik. Abo: Dataset and benchmarks for real-world 3d object understanding. In *CVPR*, 2022. 2
- [6] Manuel Contero, David Pérez-López, Pedro Company, and Jorge D. Camba. A quantitative analysis of parametric cad model complexity and its relationship to perceived modeling complexity. *Advanced Engineering Informatics*, 56, 2023. 2
- [7] Matt Deitke, Dustin Schwenk, Jordi Salvador, Luca Weihs, Oscar Michel, Eli VanderBilt, Ludwig Schmidt, Kiana Ehsani, Aniruddha Kembhavi, and Ali Farhadi. Objaverse: A universe of annotated 3d objects. In *CVPR*, 2023. 2, 3, 7
- [8] Wen-Hui Du and Francis JM Schmitt. On the g1 continuity of piecewise bézier surfaces: a review with new results. *Computer-Aided Design*, 1990. 5
- [9] Elona Dupont, Kseniya Cherenkova, Dimitrios Mallis, Gleb Gusev, Anis Kacem, and Djamila Aouada. Transcad: A hierarchical transformer for cad sequence inference from point clouds. In *ECCV*, 2024. 3
- [10] Patrick Esser, Sumith Kulal, Andreas Blattmann, Rahim Entezari, Jonas Müller, Harry Saini, Yam Levi, Dominik Lorenz, Axel Sauer, Frederic Boesel, et al. Scaling rectified flow transformers for high-resolution image synthesis. In *ICML*, 2024. 2, 6
- [11] Gerald Farin. *Curves and surfaces for CAGD: a practical guide*. Morgan Kaufmann Publishers Inc., San Francisco, CA, USA, 5th edition, 2001. 2
- [12] James D. Foley, Andries van Dam, Steven K. Feiner, and John F. Hughes. *Computer graphics: principles and practice (2nd ed.)*. Addison-Wesley Longman Publishing Co., Inc., USA, 1990. 2
- [13] Huan Fu, Rongfei Jia, Lin Gao, Mingming Gong, Binqiang Zhao, Steve Maybank, and Dacheng Tao. 3d-future: 3d furniture shape with texture. *IJCV*, 2021. 2, 5, 6
- [14] Prashant Govindarajan, Davide Baldelli, Jay Pathak, Quentin Fournier, and Sarath Chandar. Cadmium: Fine-tuning code language models for text-driven sequential cad design. *arXiv:2507.09792*, 2025. 3
- [15] Haoxiang Guo, Shilin Liu, Hao Pan, Yang Liu, Xin Tong, and Baining Guo. Complexgen: Cad reconstruction by b-rep chain complex generation. *SIGGRAPH*, 2022. 2, 3, 14
- [16] Edward J Hu, yelong shen, Phillip Wallis, Zeyuan Allen-Zhu, Yuanzhi Li, Shean Wang, Lu Wang, and Weizhu Chen. LoRA: Low-rank adaptation of large language models. In *ICLR*, 2022. 7, 9
- [17] Bonsa Hunde and Abraham Woldeyohannes. Future prospects of computer-aided design (cad) – a review from the perspective of artificial intelligence (ai), extended reality, and 3d printing. *Results in Engineering*, 2022. 2
- [18] Pradeep Kumar Jayaraman, Aditya Sanghi, Joseph G. Lambourne, Karl D.D. Willis, Thomas Davies, Hooman Shayani, and Nigel Morris. Uv-net: Learning from boundary representations. In *CVPR*, 2021. 3
- [19] Benjamin Jones, Dalton Hildreth, Duowen Chen, Ilya Baran, Vladimir G Kim, and Adriana Schulz. Automate: A dataset and learning approach for automatic mating of cad assemblies. *SIGGRAPH*, 2021. 2, 3, 5, 6
- [20] Mohammad Sadil Khan, Elona Dupont, Sk Aziz Ali, Kseniya Cherenkova, Anis Kacem, and Djamila Aouada. Cad-signet: Cad language inference from point clouds using layer-wise sketch instance guided attention. In *CVPR*, 2024. 3
- [21] Mohammad Sadil Khan, Sankalp Sinha, Sheikh Talha Uddin, Didier Stricker, Sk Aziz Ali, and Muhammad Zeshan Afzal. Text2cad: Generating sequential CAD designs from beginner-to-expert level text prompts. In *NeurIPS*, 2024. 2, 3, 5, 7
- [22] Mukul Khanna, Yongsen Mao, Hanxiao Jiang, Sanjay Haresh, Brennan Shacklett, Dhruv Batra, Alexander Clegg, Eric Undersander, Angel X Chang, and Manolis Savva. Habitat synthetic scenes dataset (hssd-200): An analysis of 3d scene scale and realism tradeoffs for objectgoal navigation. In *CVPR*, 2024. 2
- [23] Sebastian Koch, Albert Matveev, Zhongshi Jiang, Francis Williams, Alexey Artemov, Evgeny Burnaev, Marc Alexa, Denis Zorin, and Daniele Panozzo. Abc: A big cad model dataset for geometric deep learning. In *CVPR*, 2019. 2, 3, 5, 6, 7
- [24] Maksim Kolodiaznyi, Denis Tarasov, Dmitrii Zhemchuzhnikov, Alexander Nikulin, Ilya Zisman, Anna Vorontsova, Anton Konushin, Vladislav Kurenkov, and

- Danila Rukhovich. cadrille: Multi-modal cad reconstruction with online reinforcement learning. *arXiv:2505.22914*, 2025. 7
- [25] Black Forest Labs. Flux. <https://github.com/black-forest-labs/flux>, 2024. 6
- [26] Joseph G. Lambourne, Karl D.D. Willis, Pradeep Kumar Jayaraman, Aditya Sanghi, Peter Meltzer, and Hooman Shayani. Brepnet: A topological message passing system for solid models. In *CVPR*, 2021. 2
- [27] Mingi Lee, Dongsu Zhang, Clément Jambon, and Young Min Kim. Brepdiff: Single-stage b-rep diffusion model. In *Proceedings of the Special Interest Group on Computer Graphics and Interactive Techniques Conference Conference Papers*, 2025. 3, 7
- [28] Jeremy Li. Applications of computer-aided design technology in research, engineering and industry. *Computer Aided Design: Technology, Types and Practical Applications*, 2012. 1
- [29] Jiahao Li, Hao Tan, Kai Zhang, Zexiang Xu, Fujun Luan, Yinghao Xu, Yicong Hong, Kalyan Sunkavalli, Greg Shakhnarovich, and Sai Bi. Instant3d: Fast text-to-3d with sparse-view generation and large reconstruction model. In *ICLR*, 2024. 6
- [30] Jing Li, Yihang Fu, and Falai Chen. Dtgbreppen: A novel b-rep generative model through decoupling topology and geometry. In *CVPR*, 2025. 3
- [31] Jiahao Li, Weijian Ma, Xueyang Li, Yunzhong Lou, Guichun Zhou, and Xiangdong Zhou. Cad-llama: Leveraging large language models for computer-aided design parametric 3d model generation. In *CVPR*, 2025. 3
- [32] Pu Li, Jianwei Guo, Xiaopeng Zhang, and Dong-Ming Yan. Secad-net: Self-supervised cad reconstruction by learning sketch-extrude operations. In *CVPR*, 2023. 3
- [33] Weiyu Li, Xuanyang Zhang, Zheng Sun, Di Qi, Hao Li, Wei Cheng, Weiwei Cai, Shihao Wu, Jiarui Liu, Zihao Wang, et al. Step1x-3d: Towards high-fidelity and controllable generation of textured 3d assets. *arXiv:2505.07747*, 2025. 4
- [34] Yaron Lipman, Ricky T. Q. Chen, Heli Ben-Hamu, Maximilian Nickel, and Matthew Le. Flow matching for generative modeling. In *ICLR*, 2023. 5
- [35] Yujia Liu, Anton Obukhov, Jan Dirk Wegner, and Konrad Schindler. Point2cad: Reverse engineering cad models from 3d point clouds. In *CVPR*, 2024. 2, 3, 14
- [36] Ilya Loshchilov and Frank Hutter. Decoupled weight decay regularization. In *ICLR*, 2019. 6
- [37] Tiange Luo, Chris Rockwell, Honglak Lee, and Justin Johnson. Scalable 3d captioning with pretrained models. In *NeurIPS*, 2023. 3, 5
- [38] Chaofan Lv and Jinsong Bao. Cadinstruct: A multimodal dataset for natural language-guided cad program synthesis. *Computer-Aided Design*, 2025. 3
- [39] Dimitrios Mallis, Ali Sk Aziz, Elona Dupont, Kseniya Cherenkova, Ahmet Serdar Karadeniz, Mohammad Sadil Khan, Anis Kacem, Gleb Gusev, and Djamila Aouada. Sharp challenge 2023: Solving cad history and parameters recovery from point clouds and 3d scans. overview, datasets, metrics, and baselines. In *ICCVw*, 2023. 2
- [40] B Mildenhall, PP Srinivasan, M Tancik, JT Barron, R Ramamoorthi, and R Ng. Nerf: Representing scenes as neural radiance fields for view synthesis. In *ECCV*, 2020. 2
- [41] John Willard Milnor and David W Weaver. *Topology from the differentiable viewpoint*. Princeton university press, 1997. 5
- [42] Andrew Nealen, Takeo Igarashi, Olga Sorkine, and Marc Alexa. Laplacian mesh optimization. In *Proceedings of the 4th International Conference on Computer Graphics and Interactive Techniques in Australasia and Southeast Asia*, 2006. 5
- [43] Onshape Inc. Onshape: Cloud-based cad platform. <https://www.onshape.com/>, 2024. 3
- [44] Open Cascade SAS. Opencascade technology (occt). <https://www.opencascade.com/open-cascade-technology/>, 2024. 2
- [45] OpenAI. Gpt-5. <https://openai.com/gpt-5/>, 2025. 5
- [46] Maxime Oquab, Timothée Darcet, Theo Moutakanni, Huy V. Vo, Marc Szafraniec, Vasil Khalidov, Pierre Fernandez, Daniel Haziza, Francisco Massa, Alaaeldin El-Nouby, Russell Howes, Po-Yao Huang, Hu Xu, Vasu Sharma, Shang-Wen Li, Wojciech Galuba, Mike Rabbat, Mido Assran, Nicolas Ballas, Gabriel Synnaeve, Ishan Misra, Herve Jegou, Julien Mairal, Patrick Labatut, Armand Joulin, and Piotr Bojanowski. Dinov2: Learning robust visual features without supervision. *arXiv:2304.07193*, 2023. 4, 5
- [47] Jeong Joon Park, Peter Florence, Julian Straub, Richard Newcombe, and Steven Lovegrove. DeepSDF: Learning continuous signed distance functions for shape representation. In *CVPR*, 2019. 2
- [48] Charles Ruizhongtai Qi, Li Yi, Hao Su, and Leonidas J Guibas. Pointnet++: Deep hierarchical feature learning on point sets in a metric space. *NeurIPS*, 2017. 6
- [49] Daxuan Ren, Jianmin Zheng, Jianfei Cai, Jiatong Li, and Junzhe Zhang. Extrudenet: Unsupervised inverse sketch-and-extrude for shape parsing. In *ECCV*, 2022. 3
- [50] Danila Rukhovich, Elona Dupont, Dimitrios Mallis, Kseniya Cherenkova, Anis Kacem, and Djamila Aouada. Cad-recode: Reverse engineering cad code from point clouds. In *ICCV*, 2025. 3, 7
- [51] Gopal Sharma, Difan Liu, Subhransu Maji, Evangelos Kalogerakis, Siddhartha Chaudhuri, and Radomír Měch. Parsenet: A parametric surface fitting network for 3d point clouds. In *ECCV*, 2020. 3, 14
- [52] Yawar Siddiqui, Tom Monnier, Filippos Kokkinos, Mahendra Kariya, Yanir Kleiman, Emilien Garreau, Oran Gafni, Natalia Neverova, Andrea Vedaldi, Roman Shapovalov, and David Novotny. Meta 3d assetgen: Text-to-mesh generation with high-quality geometry, texture, and pbr materials. In *NeurIPS*, 2024. 3, 6
- [53] Sankalp Sinha, Mohammad Sadil Khan, Muhammad Usama, Shino Sam, Didier Stricker, Sk Aziz Ali, and Muhammad Zeshan Afzal. Marvel-40m+: Multi-level visual elaboration for high-fidelity text-to-3d content creation. In *CVPR*, 2025. 3, 5, 6, 7, 13

- [54] Stefan Stojanov, Anh Thai, and James M. Rehg. Using shape to categorize: Low-shot learning with an explicit shape bias. In *CVPR*, 2021. 2, 6
- [55] Muhammad Usama, Mohammad Sadil Khan, Didier Stricker, and Muhammad Zeshan Afzal. Nurbgen: High-fidelity text-to-cad generation through llm-driven nurbs modeling. In *AAAI*, 2026. 2, 3, 7, 9, 14
- [56] Mikaela Angelina Uy, Yen yu Chang, Minhyuk Sung, Purvi Goel, Joseph Lambourne, Tolga Birdal, and Leonidas Guibas. Point2cyl: Reverse engineering 3d objects from point clouds to extrusion cylinders. In *CVPR*, 2022. 3
- [57] Ruiyu Wang, Yu Yuan, Shizhao Sun, and Jiang Bian. Text-to-cad generation through infusing visual feedback in large language models. In *ICML*, 2025. 7
- [58] Siyu Wang, Cailian Chen, Xinyi Le, Qimin Xu, Lei Xu, Yanzhou Zhang, and Jie Yang. Cad-gpt: Synthesising cad construction sequence with spatial reasoning-enhanced multimodal llms. In *AAAI*, 2025. 3
- [59] Zhengren Wang. 3d representation methods: A survey. *arXiv:2410.06475*, 2024. 2
- [60] Karl D. D. Willis, Yewen Pu, Jieliang Luo, Hang Chu, Tao Du, Joseph G. Lambourne, Armando Solar-Lezama, and Wojciech Matusik. Fusion 360 gallery: A dataset and environment for programmatic cad construction from human design sequences. *SIGGRAPH*, 2021. 2, 3, 5
- [61] Markus Worchel and Marc Alexa. Differentiable rendering of parametric geometry. *SIGGRAPH*, 2023. 3, 4
- [62] Rundi Wu, Chang Xiao, and Changxi Zheng. Deepcad: A deep generative network for computer-aided design models. In *ICCV*, 2021. 2, 3, 7
- [63] Tong Wu, Guandao Yang, Zhibing Li, Kai Zhang, Ziwei Liu, Leonidas Guibas, Dahua Lin, and Gordon Wetzstein. Gpt-4v(ision) is a human-aligned evaluator for text-to-3d generation. In *CVPR*, 2024. 7
- [64] Zhirong Wu, Shuran Song, Aditya Khosla, Fisher Yu, Linguang Zhang, Xiaoou Tang, and Jianxiong Xiao. 3d shapenets: A deep representation for volumetric shapes. In *CVPR*, 2015. 2, 5
- [65] Jianfeng Xiang, Zelong Lv, Sicheng Xu, Yu Deng, Ruicheng Wang, Bowen Zhang, Dong Chen, Xin Tong, and Jiaolong Yang. Structured 3d latents for scalable and versatile 3d generation. In *CVPR*, 2025. 2, 4, 5, 14
- [66] Haoyang Xie and Feng Ju. Text-to-cadquery: A new paradigm for cad generation with scalable large model capabilities. *arXiv:2505.06507*, 2025. 3, 7
- [67] Xiang Xu, Joseph Lambourne, Pradeep Jayaraman, Zhengqing Wang, Karl Willis, and Yasutaka Furukawa. Breppen: A b-rep generative diffusion model with structured latent geometry. *SIGGRAPH*, 2024. 2, 3
- [68] An Yang, Anfeng Li, Baosong Yang, Beichen Zhang, Binyuan Hui, Bo Zheng, Bowen Yu, Chang Gao, Chengen Huang, Chenxu Lv, et al. Qwen3 technical report. In *Arxiv*, 2025. 9
- [69] Yang You, Mikaela Angelina Uy, Jiaqi Han, Rahul Thomas, Haotong Zhang, Yi Du, Hansheng Chen, Francis Engelmann, Suya You, and Leonidas Guibas. Img2cad: Reverse engineering 3d cad models from images through vlm-assisted conditional factorization. *arXiv:2408.01437*, 2024. 2
- [70] Longwen Zhang, Ziyu Wang, Qixuan Zhang, Qiwei Qiu, Anqi Pang, Haoran Jiang, Wei Yang, Lan Xu, and Jingyi Yu. Clay: A controllable large-scale generative model for creating high-quality 3d assets. *SIGGRAPH*, 2024. 3, 6
- [71] Zibo Zhao, Zeqiang Lai, Qingxiang Lin, Yunfei Zhao, Haolin Liu, Shuhui Yang, Yifei Feng, Mingxin Yang, Sheng Zhang, Xianghui Yang, et al. Hunyuan3d 2.0: Scaling diffusion models for high resolution textured 3d assets generation. *CoRR*, 2025. 2, 4
- [72] Shengdi Zhou, Tianyi Tang, and Bin Zhou. Cadparser: a learning approach of sequence modeling for b-rep cad. In *IJCAI*, 2023. 2, 3, 5
- [73] Qiang Zou, Yingcai Wu, Zhenyu Liu, Weiwei Xu, and Shuming Gao. Intelligent cad 2.0. *Visual Informatics*, 2024. 1



In Figures 12, 13, and 14, we present representative examples of the generated captions. In Figure 12 (top), captions for complex shapes are shown, where our pipeline produces highly detailed descriptions such as “*Stem-shaped connector ... six leaf-like fins*” or “*AM14U3 end sheet ... 39 circular holes.*” In Figure 12 (bottom), we highlight the effect of metadata inclusion, especially part names, which significantly improves the specificity of captions for simpler shapes. For example, cases 3, 4, and 8 demonstrate that visually similar ring-like structures are correctly identified as “*Valve Stem Washer,*” “*LV Bushing Washer,*” and “*Inductive Sensor Washer,*” respectively. Such fine-grained captions are essential because many small components in larger assemblies are geometrically simple. In Figure 13, we present captions that distinguish between different screw and bolt types (e.g., *M1.2, M2, M10*) as well as variations in length for the same bolt type (e.g., *M3×8, M3×14*). Finally, Figure 14 illustrates captions generated for letter-based or engraving-style CAD models.

## 10. More Experimental Results

VAE	Sparse	Coarse		Fine-Grained	
	Structure	Image	Point	Image	Point
71M	133M	354M	280M	400M	325M

Table 5. Parameter counts for all components of DreamCAD.

**A. Training Details:** For VAE training, we adopt the same weight initialization scheme and KL weighting as in Trelis [65]. The output layer predicting the deformation vector is initialized with  $N(0, 10^{-5})$ , and the control-point weight prediction layer is zero-initialized with its bias set to 1. This initialization encourages the model to produce only minimal deformations in the early stages, substantially reducing the likelihood of unstable spikes or surface artifacts compared to random initialization. Since DreamCAD must handle CAD models with widely varying geometric complexity, it is important that the VAE is trained on a diverse set of patch configurations. To provide an overview of this variability, Figure 11 shows the distribution of Bézier patch counts across the training samples.

For both the coarse and fine-grained Flow Transformers, we use 12 Transformer decoder layers. The flow-matching models are trained using a logit-normal time schedule with  $\mu=0$  and  $\sigma=1$ , and optimized with AdamW using a learning rate of  $5 \times 10^{-5}$ . Table 5 lists the number of parameters for all the modules in the DreamCAD pipeline.

**B. Conditional Generation Results:** Figure 15, 16, 17, 18 provide additional qualitative results for conditional CAD generation across all modalities - *points, images, and texts*.

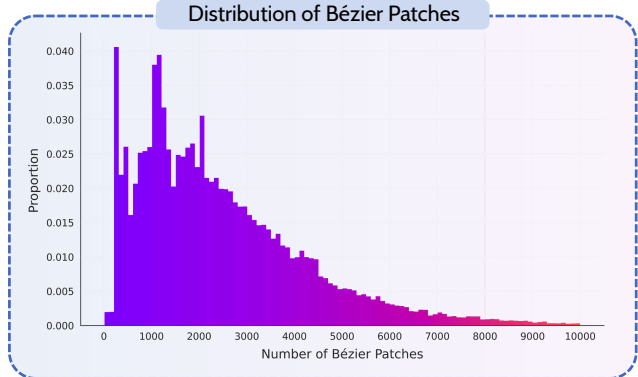


Figure 11. Distribution of patch sizes in training datasets.

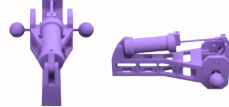
## 11. Discussion on Future Research Direction

DreamCAD addresses the first and one of most challenging stages of scalable CAD generation: learning accurate geometric reconstruction from large-scale unstructured 3D data without CAD-specific annotations. A natural question is whether *patch-based parametric surfaces are sufficient for real industrial workflows*. We argue that patch-based surfaces are not the final goal, but rather a necessary and tractable foundation.

Our key insight is that while recovering CAD topology remains a challenging problem in its own right, jointly generating geometry and topology from multimodal inputs at scale is a harder problem. The former can leverage decades of reverse engineering research [1, 15], well-defined geometric primitives [55], and existing fitting tools [35, 51]. The latter requires simultaneous reasoning over noisy inputs, diverse 3D geometries, and complex topological structure, with no comparable infrastructure to draw upon. As a first step toward topology recovery, our experiment in Section 5.4 DreamCAD’s outputs can be converted into production-level CAD models.

# CADCap -1M

## Complex Shapes

 <p><b>Stem-shaped connector</b> with central threaded cylinder, four curved arms, six leaf-like fins, three looped hooks, and one angled <b>tubular outlet</b>. Length slightly exceeds height.</p>	 <p><b>Fuel pump housing</b>, cylindrical with central cap, radial flange, two perpendicular nozzles, and base bracket featuring two bolt holes. Width and height are similar.</p>	 <p><b>Motor controller housing</b>, rectangular base (width:length <math>\approx 0.8</math>) with fourteen holes, raised cylindrical bosses, fins, posts, and filleted edges; features arranged perpendicular and parallel to base.</p>	 <p><b>Impeller wheel</b> with radial blades, conical hub, and one central bore. Wide profile: width and length are 2.5 times height.</p>
 <p><b>Elbow pipe fitting</b> with cylindrical barb and threaded male end, hexagonal nut section, and smooth 90-degree bend. Height-to-width ratio about 1.9.</p>	 <p>Wide mechanical linkage assembly with cylindrical <b>actuator</b>, triangular side frames, two circular <b>eyelets</b>, multiple rectangular <b>cutouts</b>, and parallel rods connecting pivoting end brackets. Features multi-axis joints, reinforcing ribs, and mixed prismatic and cylindrical interfaces enabling articulated motion. Likely designed for load-bearing or motion transfer applications.</p>	 <p>Tall cylindrical <b>fastener</b> with single central hole, ribbed midsection, flanged head, <b>hexagonal</b> nut end, and one perpendicular side tab. Height greatly exceeds width and length.</p>	 <p><b>AM14U3</b> end sheet bracket: wide rectangular U-channel profile with perpendicular flanges. Contains <b>39</b> circular <b>holes</b> ... across both flanges. Length is 3.1 times height and twice the width. <b>Filleted</b> outer corners: ...</p>

## Complex Prompts for Simple Shapes

 <p><b>Cylindrical adapter</b> with concentric stepped diameters and smooth fillets; squat profile (height is half the width), no holes or slots.</p>	 <p><b>Handle backer plate</b>, long rectangular bar without holes; extremely wide length-to-height ratio of 13.3:1.</p>	 <p><b>Valve Stem Washer</b>: flat circular washer with one concentric through-hole; uniform thickness and smooth outer rim.</p>	 <p><b>LV bushing washer</b>: flat circular ring with one central through-hole, uniform thickness, concentric inner and outer diameters, slight edge fillets.</p>
 <p><b>Side gusset plates</b>: wide rectangular plates with slight tapered bottom edges, no holes or ribs. Height is 10 times the width.</p>	 <p>Flat rectangular <b>door panel</b>, extremely wide relative to length (width-to-length 26.7), uniform thickness, no holes, slots, or edge features.</p>	 <p><b>Half floor sheet</b>: flat rectangular plate, very thin profile, no holes or features, sharp square corners, parallel top and bottom faces.</p>	 <p>Inductive <b>sensor washer</b>: cylindrical ring shape with one concentric through-hole, uniform thickness, smooth edges.</p>

Figure 12. Examples of generated captions for **complex** (top) and **simple** (bottom) CAD parts.

# CADCap -1M

## M3 bolts (Different Length)

 <p>Cylindrical <b>M3x8</b> bolt with straight shank and round flange head; concentric features, smooth fillets. Height is twice the width.</p>	 <p><b>M3x14</b> bolt with cylindrical shank and round head; simple, smooth geometry without threads. Length-to-height ratio approximately 0.4.</p>	 <p><b>M3x30</b> bolt. Tall cylindrical fastener with a straight shank and a single circular head. Height is 5.5 times the width. Head is concentric with the shank; ends are flat and perpendicular to the axis.</p>	 <p><b>M3x35</b> bolt, tall cylindrical shank with flat circular head; height is 6.4 times the width.</p>
--	--	---	--

## Screw

 <p><b>M1.2</b> countersink screw with cylindrical shank, flat slotted head, and shallow conical underside. Height is 2.1 times length; width is half height.</p>	 <p><b>M2</b> screw with cylindrical threaded shank and domed pan head featuring a single Phillips cross recess; wide profile (width-to-height 2.4).</p>	 <p><b>M2.5-10</b> bolt with cylindrical shank and round pan head featuring a single cruciform screwdriver slot.</p>	 <p><b>M3x8</b> screw with cylindrical shank and broad round head featuring a single cross slot; length-to-height ratio 0.6.</p>
 <p>Hexagon socket head cap screw with cylindrical head, central hex recess, and long threaded shank; concentric features, ISO 4762 <b>M5 x 20</b>.</p>	 <p>DIN912 <b>M6</b> socket head cap screw; tall cylindrical shank with round head and central hexagonal socket. Height is 2.4x length.</p>	 <p><b>M8x12</b> cylindrical fastener with round head, hexagonal socket recess, and straight shank. Width to length ratio is 1.3.</p>	 <p>Bolt with cylindrical shank and round head, featuring a central hex socket and concentric faces. <b>M10 x 30</b>.</p>

Figure 13. Examples of generated captions for different types of **fasteners**.

## CADCap-1M

### Letter-Shape



Wide A-shaped structural bracket with single central rectangular hole, internal ribs, and tapered legs; height is 1.1x length and 4.4x width.



C-shaped fork bracket with cylindrical stem, semicircular arms, two inner grooves, and rounded ends; stem concentric and perpendicular to fork.



D-shaped ring connector, rounded outer profile with one internal opening (one hole). Thick, uniform cross-section; flat bottom, semicircular top.



Tall K-shaped mounting bracket with four circular holes and a perpendicular rectangular flange; height is 4.7 times length.



L-shaped mounting bracket with semicircular end, ten circular holes including central bores on both faces. Nearly square proportions; perpendicular legs with concentric hole patterns.



Wide T-shaped bracket with very long stem and three circular holes; two on crossbar, one at stem end. Width-to-height ratio 34:1.

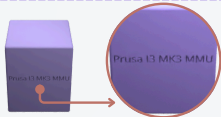


U-shaped rod bracket with uniform round cross-section, smooth curved top, and two parallel straight legs. Length is 7.6 times width.



Forked Y-shaped bracket, extremely long length-to-height 17:1. Two small circular holes near base, parallel tapered arms with open end.

### Engravings



Rectangular housing block with smooth faces, slight edge fillets, and embossed "Prusa I3 MK3 MMU" text on one side.



Lettering plate forming "BMO" text, flat and wide. One through-hole within the "O"; uniform thickness, rounded outer edges.



Rectangular nameplate, very wide (height is 0.1x width), with recessed "Danny" text on flat top face.



Flat rectangular plate with raised "lyft"-like embossed lettering on one corner; uniform thickness, smooth edges, no holes or additional features.



Rectangular sign block with 3D extruded letters "QUALITY CAMERA". Length is 2.4 times the width, displaying distinct separation between words.



Flat teardrop-shaped plate, slightly taller than long, with smooth filleted perimeter and embossed "K" marking on one face.



Conical marker pin with flat circular top and engraved "CF" lettering; single sharp apex below.



Round coin-like disk, very wide relative to height, with shallow recessed "£1" engraving on the top face. Length-to-height ratio 7.2.

Figure 14. Examples of generated captions for **letter-based** (top) and **engraving-style** (bottom) CAD models

# DreamCAD



Figure 15. More qualitative results for the *point-to-CAD* reconstruction task using DreamCAD. Each row shows input point clouds (top) and the corresponding reconstructed CAD models (bottom) generated by DreamCAD across a wide range of shapes, including mechanical components, furniture, utensils, and free-form surfaces. As seen in the examples, DreamCAD successfully recovers clean parametric geometry from input point clouds, preserving fine structural details (e.g., *tubular connectors*, *circular cutouts*, *brackets*), smooth surfaces (e.g., *bowls*, *vases*, *seats*), and complex topologies (e.g., *multi-part assemblies* and *chair frames*).

# DreamCAD



Figure 16. More qualitative results for the *image-to-CAD* generation task using DreamCAD. Each row shows the ground-truth reference image (top) and the CAD reconstruction produced by DreamCAD (bottom) across a wide range of object categories, including furniture, mechanical parts, consumer products, and free-form designs. As seen in the examples, DreamCAD consistently recovers accurate 3D geometry from a single image, capturing fine structural details (e.g., *chair backrests*, *table legs*, *nozzle openings*), complex mechanical features (e.g., *gear teeth*, *connectors*, *threads*), and overall proportions with high fidelity.



Figure 17. More qualitative *text-to-CAD* results on the test set. Each row shows an input text description (bottom) and the corresponding CAD geometry generated by DreamCAD (top). DreamCAD successfully reconstructs shapes from complex text prompts, ranging from mechanical parts (*gear assemblies, flange plates, couplings*), tools (*pyramidal axe head*), and structural elements (*DIN rail, stepped platforms*), to free-form designs (*curved hooks, seat frames, turbine blades*), and consumer objects (*USB cable*).

# DreamCAD



Figure 18. *Text-to-CAD* generation results on GPT-generated prompts. Each example shows a text prompt produced by GPT-5 (bottom) and the corresponding CAD reconstruction (top) by DreamCAD. As shown, DreamCAD generalizes beyond dataset-style prompts and reliably interprets free-form, open-vocabulary instructions which includes consumer electronics (*smartphone*, *computer mouse*), household items (*frying pan*, *stool*, *water cooler bottle*), tools (*screwdriver*, *crowbar*, *scissors*), mechanical components (*V-groove pulley*), and articulated objects (*desk lamp arm*, *quadcopter drone*).